



2950 Niles Road, St. Joseph, MI 49085-9659, USA
269.429.0300 fax 269.429.3852 hq@asabe.org www.asabe.org

An ASABE Meeting Presentation

Paper Number: 096998

Optical Properties of Bruised Apple Tissue

Renfu Lu¹, Ph.D., Supervisory Agricultural Engineer

Haiyan Cen², Graduate Assistant

Min Huang^{1,3}, Ph.D., Associate Professor

Diwan P. Ariana², Ph.D., Visiting Assistant Professor

¹USDA ARS Sugarbeet and Bean Research Unit, 224 Farrall Hall, Michigan State University, East Lansing, MI 48824

²Department of Biosystems and Agricultural Engineering, Michigan State University, East Lansing, MI 48824

³School of Communication and Control Engineering, Jiangnan University, Wuxi, China

**Written for presentation at the
2009 ASABE Annual International Meeting
Sponsored by ASABE
Grand Sierra Resort and Casino
Reno, Nevada
June 21 – June 24, 2009**

Abstract. *Understanding optical properties of apple tissue, especially bruised tissue, can help us develop an effective method for detecting bruises during sorting and grading. This research was conducted on determining the optical properties of bruised apple tissue over 500-1,000 nm and quantifying their changes with time. Spectral absorption and reduced scattering coefficients were determined from the normal, unbruised tissues of 'Golden Delicious' and 'Red Delicious' apples and then bruised tissues at different time intervals after bruising, using a hyperspectral imaging-based spatially resolved technique. Absorption for normal tissues was generally lower than that for the bruised tissues in the spectral region of less than 600 nm, while an opposite trend was observed in the spectral region of 800-1,000 nm. The reduced scattering coefficient for normal tissues was much higher than that for the bruised tissues; it decreased consistently over time. Bruising had greater impact on scattering than on absorption. Hence an optical system that can enhance scattering features would be better suited for bruise detection.*

Keywords. Apples, quality, bruises, optical properties, absorption, scattering, hyperspectral imaging, diffuse reflectance, spatially resolved.

The authors are solely responsible for the content of this technical presentation. The technical presentation does not necessarily reflect the official position of the American Society of Agricultural and Biological Engineers (ASABE), and its printing and distribution does not constitute an endorsement of views which may be expressed. Technical presentations are not subject to the formal peer review process by ASABE editorial committees; therefore, they are not to be presented as refereed publications. Citation of this work should state that it is from an ASABE meeting paper. EXAMPLE: Author's Last Name, Initials. 2009. Title of Presentation. ASABE Paper No. 09----. St. Joseph, Mich.: ASABE. For information about securing permission to reprint or reproduce a technical presentation, please contact ASABE at rutter@asabe.org or 269-429-0300 (2950 Niles Road, St. Joseph, MI 49085-9659 USA).

Introduction

Apple bruising frequently occurs during harvest, postharvest handling, transport, and retailing and it is of great concern because bruised apples can be downgraded or even rejected by consumers, which would result in economic loss to growers, packers, shippers or retailers. Hence preventing or minimizing bruise occurrence at various harvest and postharvest operations is utmost important. Moreover, it is also critical to have an effective inspection system to segregate those apples with pre-existing quality-degrading bruises from premium quality ones during sorting and grading.

A large volume of literature exists on mechanical properties of fruit tissue, bruising mechanisms, and bruise prevention, mitigation and detection methods (Abbott et al., 1997; Bajema and Hyde, 1998; Garcia-Ramos et al., 2003; Mohsenin, 1986; Shahin et al., 2002; Van Zeebroeck et al., 2007). Bruises are primarily caused by two types of mechanical load, i.e., static and dynamic (Mohsenin, 1986). Excessive static load may be exerted on apples in large containers during shipment and storage. Most apple bruises, however, are caused by dynamic load in the form of vibration or impact. Impact bruising is the most common, and it occurs frequently in harvest, transport, and postharvest handling and sorting/grading (Baritelle and Hyde, 2001).

After an apple fruit is bruised, the moisture content of the bruised tissue will increase initially. As time progresses, the bruised tissue starts to lose moisture. These changes are accompanied with changes in the tissue physical and chemical properties. Lu (2003) reported that reflectance for bruised tissue over the near-infrared region of 900-1,300 nm was lower than that for normal tissue during the initial period after bruising, which was primarily attributed to increases in the moisture content and perhaps also soluble solids content in the bruised tissue. Thereafter, reflectance of the bruised tissue became higher than that of normal tissue. Currently spectral imaging at single or multiple wavebands is being used for defect detection of fruits and vegetables. Other imaging techniques, such as hyperspectral imaging (Ariana et al., 2006; Lu, 2003), also have been explored for bruise detection. These optical imaging techniques achieve bruise detection via ascertaining or evaluating the changes or differences in optical characteristics (i.e., reflectance and transmittance) between normal and bruised tissues. However, reflectance and transmittance are not intrinsic properties and their measurements are often dependent on sensing configuration and type of sensor used.

Light interaction with the turbid fruit tissue involves absorption and scattering, which are characterized by the absorption (μ_a) and reduced scattering coefficients (μ_s') (Qin and Lu, 2008). Knowledge of the optical properties will enable us to gain insight about the interaction of light with the fruit tissue, which would be valuable in the development of an optical technique for evaluating properties and characteristics that are indicative of specific quality attributes or defects such as bruises. Until recently, it has been a great challenge to measure the absorption and scattering properties of fruits and food products because they are intertwined and difficult to separate. Several studies (Anderson et al., 2007; Cubeddu et al., 2001; Qin and Lu, 2006, 2007) were reported recently on using new techniques to measure horticultural and food products. Among them is hyperspectral imaging-based spatial resolved technique (Qin and Lu, 2007, 2008). This technique is simpler, faster, and relatively easier to use, compared to time resolved, frequency domain, and spatial frequency domain techniques (Anderson et al., 2007; Cubeddu et al., 2001). Anderson et al. (2007) applied spatial frequency technique to measure the optical properties of normal and bruised apple tissues. They demonstrated that the technique could be used to detect bruises on apples because bruised tissue had lower values in the absorption and reduced scattering coefficients than normal tissue. However, Anderson et al. (2007) only reported results for two 'Golden Delicious' apples and provided no further

information on how other factors, such as degree of bruising, bruise age, etc., may affect the optical properties. To better understand optical characteristics of bruised tissue, it is necessary to quantify the absorption and scattering properties and their changes with time.

Therefore the objectives of this research were to:

- Measure the absorption and reduced scattering coefficients for normal and bruised apple tissues using a hyperspectral imaging-based spatially resolved technique for the visible and near-infrared region of 500-1,000 nm;
- Quantify the changes of absorption and scattering properties for bruised apple tissues over time.

Materials and Methods

Hyperspectral Imaging System

A line-scan (or pushbroom) hyperspectral imaging system, developed at the U.S. Department of Agriculture Agricultural Research Service (USDA/ARS) postharvest engineering lab at Michigan State University, East Lansing, MI, was used to measure the optical properties of normal and bruised apple tissues (Fig. 1).

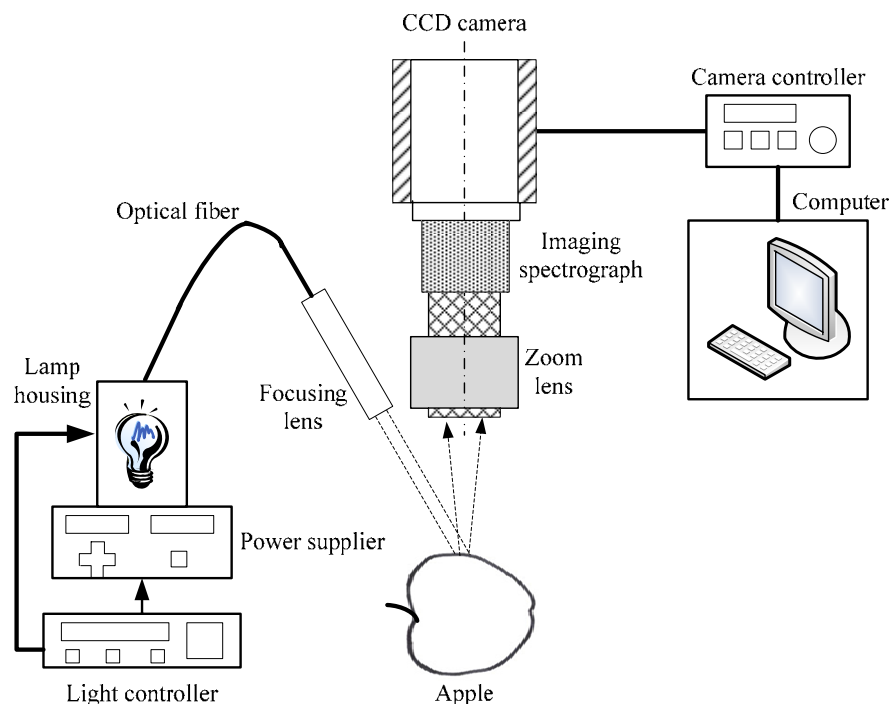


Figure 1. Hyperspectral imaging system for acquiring spatially resolved scattering images from apples.

This system was made up of a back-illuminated 512×512-pixel CCD (charge-coupled device) camera (Model C4880-21-24A, Hamamatsu Corp, Bridgewater, NJ, USA) which was connected with an imaging spectrograph (V10 OEM, Specim, Finland) that had an effective spectral range of 400-1,000 nm. A single optic fiber coupled with a microlens was used to provide continuous-wave light output via a quartz tungsten halogen DC-supplied light source with a feedback control (Oriol Instruments, Stratford, CT, USA). The sample handling unit was mainly composed

of one vertical motorized stage, one horizontal motorized stage and a through-beam photoelectric sensor. Each test fruit was placed on the holder of the sample handling unit with its stem-calyx axis being horizontal and also perpendicular to the scan line of the hyperspectral imaging unit. The two stages were controlled by a computer program to automatically move the fruit to the pre-determined initial position. Once the fruit was at the initial position, it started to move horizontally in synchronization with the camera's imaging acquisition speed. The imaging system acquired 2-D spatially resolved reflectance (scattering) images generated by the 1.0 mm light beam at the surface of the sample. The 2×2 binned images had a spectral resolution of 4.54 nm per pixel along the vertical direction and a spatial resolution of 0.20 mm per pixel in the horizontal direction. The system was calibrated to compensate for nonuniform instrument response (Qin and Lu, 2007). A detailed description of the hyperspectral imaging system can be found in Qin and Lu (2008).

Experimental Procedure

Sample Preparation

Forty 'Golden Delicious' apples and 40 'Red Delicious' apples were used in the study. These apples were harvested from a research orchard of the Michigan State University Horticultural Teaching and Research Center in Holt, Michigan in 2008. The apples were kept in refrigerated air at 0 °C for about one month after harvest and before the bruise experiment was started. Each apple was visually inspected to ensure it was free from pre-existing bruises.

Bruises on the test apples were induced by impact generated from a 76 mm (3") wooden ball, weighing approximately 135 g, which was mounted onto one end of a 483 mm long aluminum rod. The other end of the rod was mounted onto a pivotal axis so that the wooden ball would act as a pendulum to turn freely around the pivotal axis. The wooden-ball pendulum was rotated upward about 40° from the horizontal direction and then released; the ball fell freely until it hit at an equatorial area of the fruit. After completion of the first impact, a second impact of the same magnitude was followed, which hit at an area adjacent to the first impact area. The total impact energy for the two impact tests was estimated to be at 0.30 joules. Impacting each apple with the wooden ball for two times was intended to create a sufficiently large bruise area (or volume) that would be needed for subsequent imaging of the bruised tissue. The average bruise size and depth were 29.0 mm and 7.4 mm for 'Golden Delicious' apples, and 30.4 mm and 8.2 mm for 'Red Delicious' apples respectively. This would ensure that scattering images (10 for each apple each time, see more details in the following section), which covered approximately a 20 x 9 mm (scanning line distance x scanning direction) area, would have been taken from the bruised areas only.

Hyperspectral Scattering Image Acquisition

Scattering images were first obtained for each unbruised fruit, providing initial information on the optical properties of normal apple tissues (denoted as day 0-). Ten scattering images were collected from the equatorial area of each fruit, covering 9 mm distance. After imaging from the unbruised apples, bruises were induced on all apples following the procedure described above. Scattering images were then acquired from each bruised apple within two to three hours after bruising (denoted as day 0+). The same imaging procedure for normal apples was followed for the bruised apples. However, special care was taken in acquiring scattering images from the bruised apples. Each sample was carefully placed on the sample holder, so that the light beam would be approximately located in the central position of the bruised area. This procedure was to ensure that scattering images would be acquired from the bruised tissue only, not from the

neighboring unbruised tissue. The bruised apples were imaged again at 1, 2, 5, 9, 16, and 23 days after bruising to determine the change of the optical properties over time. Between the dates of imaging, the apples were kept in cold storage at 2 °C. Since fruit temperature at the time of testing might affect the measurement of optical properties, all fruit were removed from cold storage and kept at room temperature (~22 °C) for at least 12 h.

Determination of Optical Properties

Diffusion Theory Model

Light transport in a turbid material is governed by radiation transfer theory. When scattering is dominant over absorption (i.e., $\mu_s' \gg \mu_a$, where μ_s' is the reduced scattering coefficient in cm^{-1} and μ_a is the absorption coefficient in cm^{-1}), light transport in the turbid material may be described by diffusion approximation theory (Mobley and Vo-Dinh, 2003). When a steady-state (or continuous wave) light beam of infinitely small size is perpendicularly incident upon a scattering-dominant semi-infinite medium, the backscattering profile, $R(r)$, at the surface of the medium is a function of distance r and μ_s' and μ_a , which may be expressed as follows (Farrell et al., 1992):

$$R(r) = \frac{a'}{4\pi} \left[\frac{1}{\mu_t'} \left(\mu_{\text{eff}} + \frac{1}{r_1} \right) \frac{\exp(-\mu_{\text{eff}} r_1)}{r_1^2} + \left(\frac{1}{\mu_t'} + \frac{4A}{3\mu_t'} \right) \left(\mu_{\text{eff}} + \frac{1}{r_2} \right) \frac{\exp(-\mu_{\text{eff}} r_2)}{r_2^2} \right] \quad (1)$$

where r is the distance from the incident point, a' is the transport albedo [$a' = \mu_s' / (\mu_a + \mu_s')$], μ_{eff} is the effective attenuation coefficient ($\mu_{\text{eff}} = [3\mu_a (\mu_a + \mu_s')]^{1/2}$), and μ_t' is the total attenuation coefficient ($\mu_t' = \mu_a + \mu_s'$). r_1 and r_2 are expressed by the following two equations:

$$r_1 = \left[\left(\frac{1}{\mu_t'} \right)^2 + r^2 \right]^{1/2} \quad (2)$$

$$r_2 = \left[\left(\frac{1}{\mu_t'} + \frac{4A}{3\mu_t'} \right)^2 + r^2 \right]^{1/2} \quad (3)$$

where A is an internal reflection coefficient determined by the mismatch of refractive indices at the interface, and it can be calculated from the empirical equations derived by Groenhuis et al. (1983).

Inverse Algorithm

As described earlier, 10 hyperspectral scattering images were acquired for each apple on each test date. To improve the signal to noise ratio and reduce the variability of individual scattering images due to the spatial variation within the imaged area of each apple, six scattering images, starting from the third image through eighth image, were averaged. The first two and the last two scattering images were excluded to ensure that the selected scattering images truly came from the bruised area of each apple.

Figure 2 shows a 2-D spatially resolved scattering image for a 'Golden Delicious' apple. This image is characterized by a spatial dimension along the horizontal axis and a spectral

dimension along the vertical axis. A horizontal line taken from the image represents a spatial scattering profile for a specific wavelength. Hence, the image consisted of more than 100 spatial scattering profiles covering the wavelengths of 500-1,000 nm.

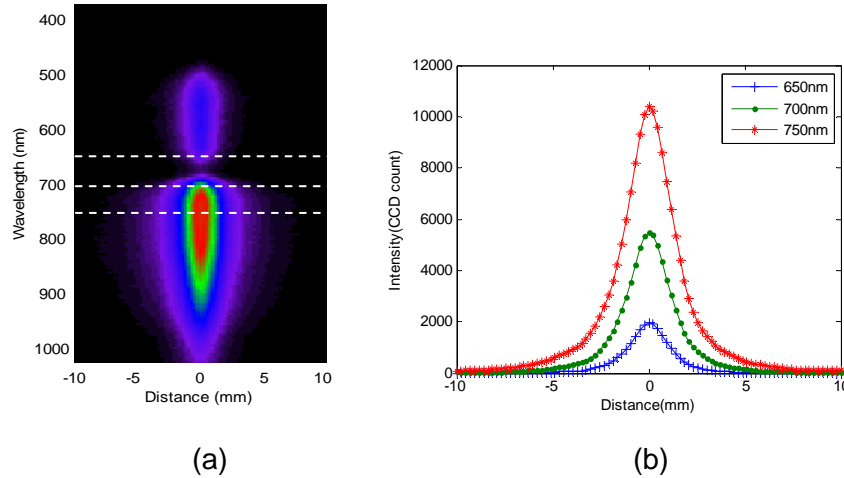


Figure 2. Hyperspectral scattering image for a 'Golden Delicious' apple: a) a 2-D image with intensity levels highlighted with pseudo colors and b) spatially resolved scattering profiles at 650 nm, 700 nm, and 750 nm.

Absorption and reduced scattering coefficients were determined from equation (1) using an inverse algorithm to fit the measured scattering profiles, as those shown in Fig. 2b. To estimate μ_a and μ_s' for each wavelength, the scattering profiles were first corrected for the fruit size and instrument nonuniformity effects. Thereafter, the profiles were averaged about the symmetric point. The averaged profiles were normalized by the peak value. The normalization process avoided the need of measuring absolute reflectance profiles. Lastly, a nonlinear trust-region least squares fitting algorithm was implemented in Matlab software (The Mathworks, Inc., Natick, MA, USA), which gave estimated values for the absorption and reduced scattering coefficients. A detailed description of the inverse algorithm for determining absorption and reduced scattering coefficients can be found in Qin and Lu (2008).

Results and Discussion

Figure 3 shows absorption and reduced scattering spectra for the normal tissues of 40 'Golden Delicious' apples for the spectral region of 500-1,000 nm (denoted as day 0-). Values of the absorption coefficient changed greatly across the spectral region. Overall, absorption in 500-700 nm was higher than that for the region of 730-900 nm (Fig. 3, left). Two absorption peaks were observed around 675 nm and 960 nm, corresponding to the absorption wavebands for chlorophylls and water. Considerable variations in absorption also existed among the test apples. Values of the reduced scattering coefficient (Fig. 3, right), on the other hand, decreased as the wavelength increased. Again, large variations in the reduced scattering coefficient were observed among the test apples. For these normal apples, values of the reduced scattering coefficient were much greater than those of the absorption coefficient. Hence scattering was dominant over absorption in the normal tissues of 'Golden Delicious' apples.

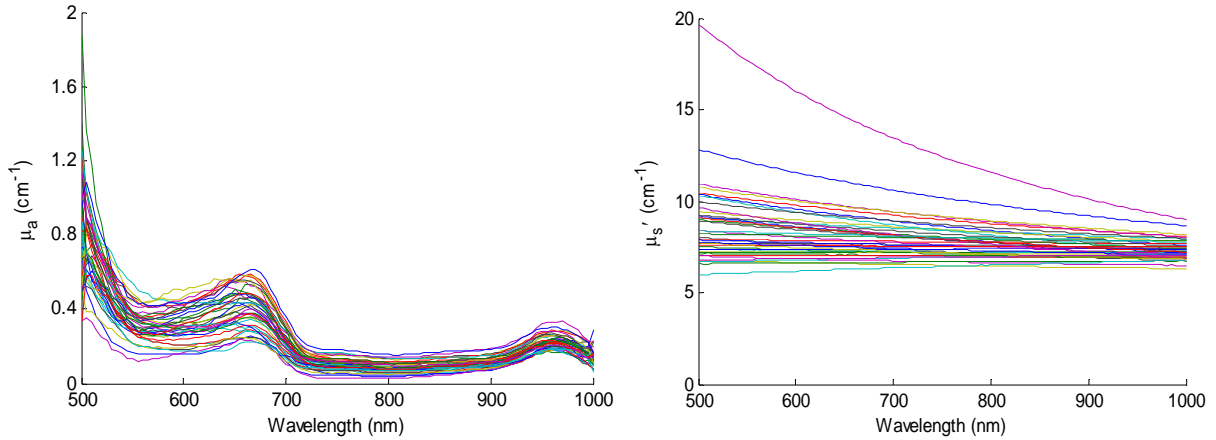


Figure 3. Absorption (left) and reduced scattering (right) coefficients for 40 normal, unbruised 'Golden Delicious' apples for the spectral region of 500-1,000 nm.

Similar trends, but somewhat different in magnitude, were noticed from the spectra of absorption and reduced scattering coefficients for the normal tissues of 'Red Delicious' apples (Fig. 4). Spectra for 'Red Delicious' apples only covered the region of 600-1,000 nm because scattering signals below 600 nm were so weak and noisy that they were not suitable for exaction of the absorption and scattering coefficients during the curve-fitting process. This also explains why absorption spectra below 670 nm for the test apples were not so consistent for 'Red Delicious' apples.

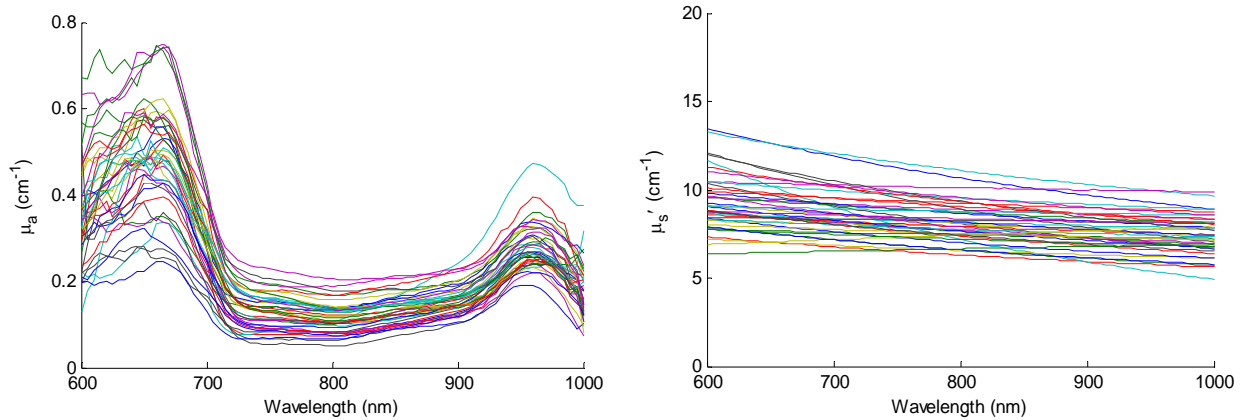


Figure 4. Absorption (left) and reduced scattering (right) coefficients for 40 normal, unbruised 'Red Delicious' apples for the spectral region of 600-1,000 nm.

To better understand the pattern of changes in the optical properties of bruised tissues over time, mean spectra of the absorption and reduce scattering coefficients for all apples were calculated for each test date. Figure 5 shows the mean spectra of absorption and reduced scattering coefficients for the normal and bruised tissues of 'Golden Delicious' apples at different dates after bruising. In the figure, label 'day 0-' denotes normal tissue, while the rest indicate results for the bruised tissue measured at specific days after bruising. Clearly, bruises had different effects on the absorption coefficient for different sections of the spectral region of 500-1,000 nm. For the region of less than 600 nm, normal tissues exhibited much lower absorption than the bruised tissues. Between the wavelengths of 600-750 nm, absorption in normal tissues was neither consistently higher nor consistently lower than for the bruised

tissues. No consistent pattern could be ascertained in this region. Beyond 800 nm, absorption for normal tissues was generally higher than that for the bruised tissues.

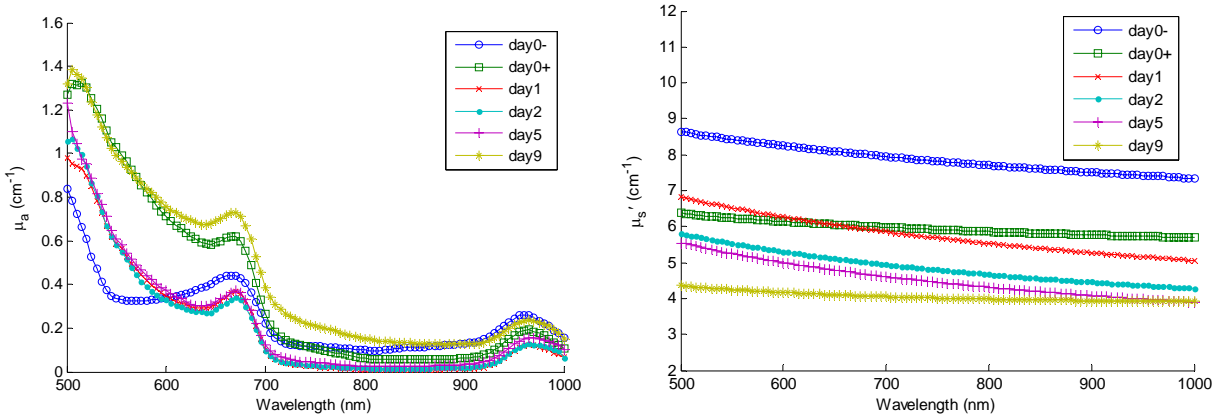


Figure 5. Mean spectra of the absorption (left) and reduced scattering (right) coefficients for the normal (day 0-) tissues and bruised tissues of 40 ‘Golden Delicious’ apples measured at different days after bruising.

Unlike the absorption coefficient, the reduced scattering coefficient exhibited a more consistent pattern of change after bruising (Fig. 5, right). Normal tissues had much higher values in the reduced scattering coefficient than the bruised tissues for all test dates. More significantly, the reduced scattering coefficient decreased consistently over time after bruising; its values at day 9 were the lowest. It should be mentioned that scattering images were also acquired for ‘Golden Delicious’ at days 16 and 23. However, results for these days are not included in Fig. 5 because the reduced scattering coefficient continued to decrease nine days after bruising. As a result, scattering was no longer dominant over absorption, which led to some erroneous or unreasonable results in estimating μ_a and μ_s' by the inverse algorithm. This is because the diffusion theory model is based on the assumption that scattering is much greater than absorption.

The overall trends of change in the absorption and reduced scattering coefficients for ‘Red Delicious’ apples (Fig. 6) were similar to those for ‘Golden Delicious’ apples. No consistent pattern of changes in the absorption coefficient between normal and bruised tissues and among the bruised tissues tested at different dates. For the reduced scattering coefficient, a consistent pattern of changes was again observed; normal tissues had much higher values in the reduced scattering coefficient than the bruised tissues. Values of the reduced scattering coefficient for the bruised tissues decreased over time and it reached the minimum at the last test date (day 23).

These results indicated that bruising had different effects on the absorption and reduced scattering coefficients. While the pattern of change for absorption between normal and bruised tissues and between the bruised tissues of different ages is difficult to quantify, a consistent pattern of change in the reduced scattering coefficient was observed. The pattern of consistent decreases in the reduced scattering coefficient for the bruised tissue over time suggests that an optical inspection system that can enhance scattering characteristics could be more effective in bruise detection.

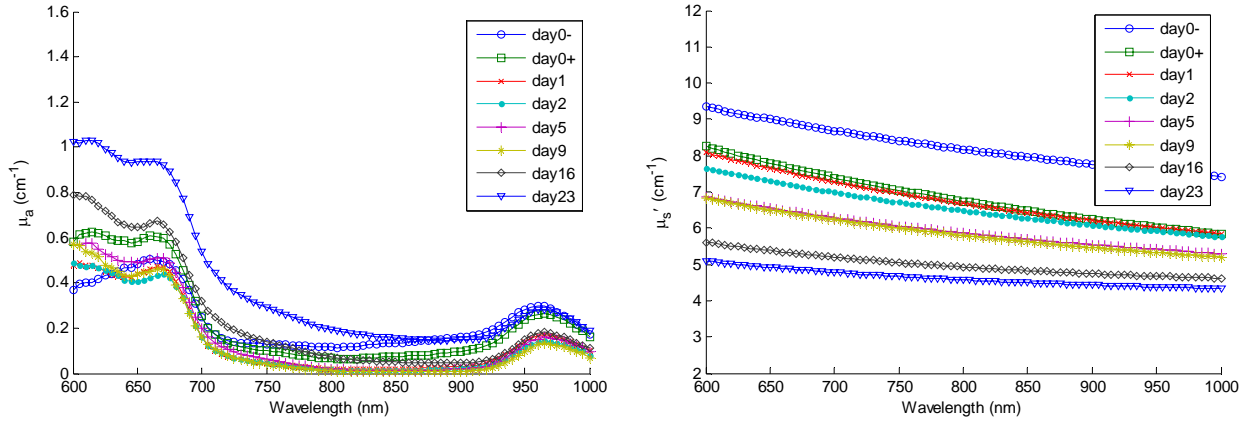


Figure 6. Mean spectra of the absorption (left) and reduced scattering (right) coefficients for the normal (day 0-) and bruised tissues of 40 'Red Delicious' apples measured at different days after bruising.

To further study the optical properties of normal and bruised tissues, the total attenuation coefficient ($\mu_t' = \mu_a + \mu_s'$) was calculated. The total attenuation coefficient reflects the attenuation or loss of light energy as it propagates in a turbid material. The pattern of change for μ_t' for 'Golden Delicious' (Fig. 7) was highly consistent; its value decreased with the increasing wavelength. Normal tissues had much higher values for μ_t' than the bruised tissues. Values of μ_t' decreased as bruises were aging. In other words, the attenuation of light was the most significant in the normal tissues and it then decreased steadily as bruises became older. Both apple varieties again had similar patterns of change for μ_t' (Figs. 7 and 8).

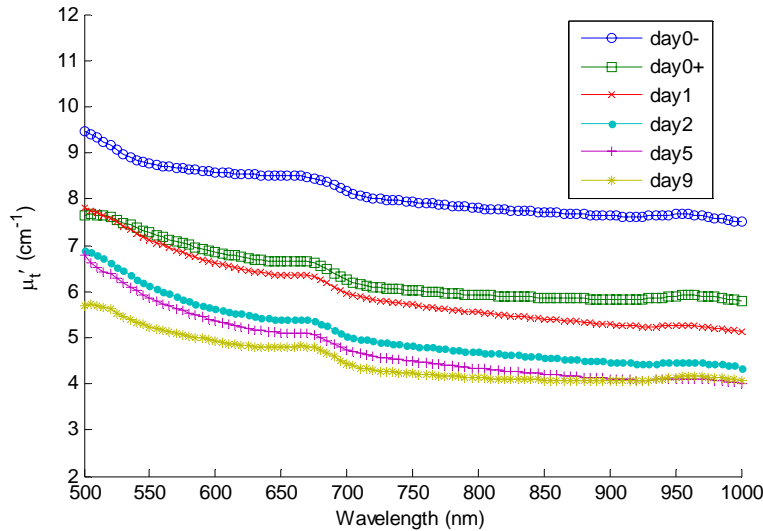


Figure 7. Mean spectra of the total attenuation coefficient for the normal (day 0-) and bruised tissues of 40 'Golden Delicious' apples measured for different days after bruising.

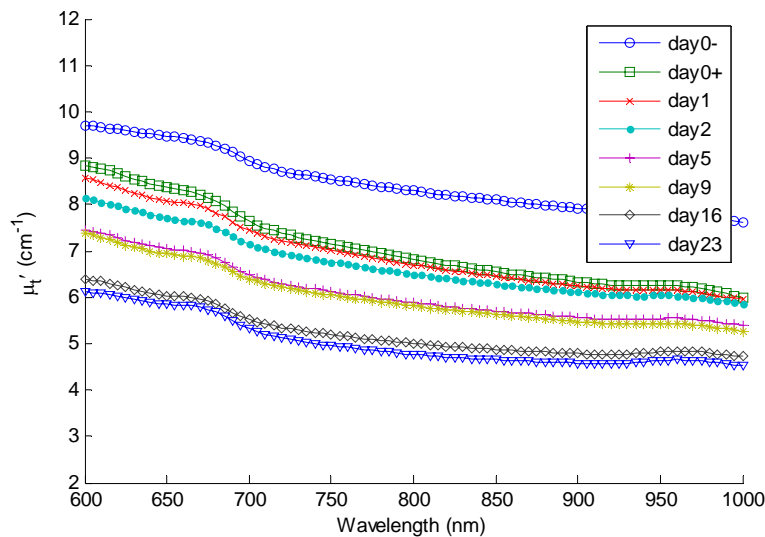


Figure 8. Mean spectra of the total attenuation coefficient for the normal (day 0-) and bruised tissues of 40 'Red Delicious' apples measured for different days after bruising.

Conclusion

This research provided new knowledge about the spectral absorption and scattering properties of normal and bruised tissues for 'Golden Delicious' and 'Red Delicious' apples and their changes with time after bruising. Bruising significantly changed the optical properties of apple tissue; however, its effects on the absorption and scattering properties were different. No consistent pattern of changes in the absorption coefficient was observed between normal and bruised tissues and between the bruised tissues of different ages. Contrarily, the reduced scattering coefficient had large drops in value after bruising and then decreased steadily over time. Light attenuation rate decreased consistently with time after the apples were bruised. These findings suggest that an optical system that can enhance scattering features may be better suited for detecting bruises on apples.

References

- Abbott, J. A., R. Lu., B. L. Upchurch, and R. L. Strohshine. 1997. Technologies for nondestructive quality evaluation of fruits and vegetables. In *Horticultural Reviews* (edited by J. Janick) 20: 1-120, John Wiley & Sons, Inc. New York.
- Anderson, E. R., D. J. Cuccia, and A. J. Durkin. 2007. Detection of bruises on Golden Delicious apples using spatially frequency-domain imaging. In *Proceedings of the SPIE*, Vol. 6430, pp. 64301O.
- Ariana, D. P., R. Lu, and D. E. Guyer. 2006. Near-infrared hyperspectral reflectance imaging for detection of bruises on pickling cucumbers. *Computers and Electronics in Agriculture* 53(1): 60-70.
- Bajema, R. W. and G. M. Hyde. 1998. Instrumented pendulum for impact characterization of whole fruit and vegetable specimens. *Transactions of the ASAE* 41(5): 1399-1405.
- Baritelle, A. L. and G. M. Hyde. 2001. Commodity conditioning to reduce impact bruising. *Postharvest Biology and Technology* 21(3): 331-339.

- Cubeddu, R., C. D'Andrea, A. Pifferi, P. Taroni, A. Torricelli, G. Valentini, M. Ruiz-Altisent, C. Valero, C. Ortiz, C. Dover, and D. Johnson. 2001. Time-resolved reflectance spectroscopy applied to the nondestructive monitoring of the internal optical properties in apples. *Applied Spectroscopy* 55(10): 1368-1374.
- Farrell, T. J., M. S. Patterson, and B. C. Wilson. 1992. A diffusion-theory model of spatially resolved, steady-state diffuse reflectance for the noninvasive determination of tissue optical properties in vivo. *Med. Physics* 19(4): 879-888.
- Garcia-Ramos, F.J., J. Ortiz-Canavate, and M. Ruiz-Altisent. 2003. Reduction of mechanical damage to apples in a packing line using mechanical devices. *Applied Engineering in Agriculture* 19(6): 703-707.
- Groenhuis, R. A. J., H. A. Ferwerda, and J. J. Bosch. 1983. Scattering and absorption of turbid materials determined from reflection measurements – 1. Theory. *Applied Optics* 22(16): 2456-2462.
- Lu, R. 2003. Detection of bruises on apples using near-infrared hyperspectral imaging. *Transactions of the ASAE* 46(2): 523-530.
- Mobley, J. and T. Vo-Dinh. 2003. Chapter 2. Optical properties of tissues. In *Biomedical Photonics Handbook* (Edited by T. Vo-Dinh), 2: 1-75. Boca Raton, FL: CRC Press.
- Mohsenin, N. N. 1986. *Physical Properties of Plant and Animal Materials*. New York, NY: Gordon and Breach Science Publishers.
- Qin, J. and R. Lu. 2006. Hyperspectral diffuse reflectance imaging for rapid, noncontact measurement of the optical properties of turbid materials. *Applied Optics* 45(32): 8366-8373.
- Qin, J. and R. Lu. 2007. Measurement of the absorption and scattering properties of turbid liquid foods using hyperspectral imaging. *Applied Spectroscopy* 61(4): 388-396.
- Qin, J. and R. Lu. 2008. Measurement of the optical properties of fruits and vegetables using spatially resolved hyperspectral diffuse reflectance imaging technique. *Postharvest Biology and Technology* 49(3): 355-365.
- Shahin, M. A., E. W. Tollner, R. W. McClendon, and H. R. Arabnia. 2002. Apple classification based on surface bruises using image processing and neural networks. *Transactions of the ASAE* 45(5): 1619-1627.
- Van Zeebroeck, M., V. Van linden, H. Ramon, J. De Baerdemaeker, B. M. Nicolai, and E. Tijskens. 2007. Impact damage of apples during transport and handling. *Postharvest Biology and Technology* 45(2): 157-167.